Published in final edited form as:

ACS Appl Mater Interfaces. 2016 December 28; 8(51): 34951–34963. doi:10.1021/acsami.6b12994.

A Review of the Fundamental Principles and Applications of Solution Blow Spinning

John L. Daristotle[†], **Adam M. Behrens**[†], **Anthony D. Sandler**[§], and **Peter Kofinas**[†,*]

[†]Fischell Department of Bioengineering, University of Maryland, 2330 Jeong H. Kim Engineering Building, College Park, Maryland 20742, United States

[§]Sheikh Zayed Institute for Pediatric Surgical Innovation Joseph E. Robert Jr. Center for Surgical Care, Children's National Medical Center, 111 Michigan Avenue NW, Washington, DC 20010, United States

Abstract

Solution blow spinning (SBS) is a technique that can be used to deposit fibers in situ at low cost for a variety of applications, which include biomedical materials and flexible electronics. This review is intended to provide an overview of the basic principles and applications of SBS. We first describe a method for creating a spinnable polymer solution and stable polymer solution jet by manipulating parameters such as polymer concentration and gas pressure. This method is based on fundamental insights, theoretical models, and empirical studies. We then discuss the unique bundled morphology and mechanical properties of fiber mats produced by SBS, and how they compare with electrospun fiber mats. Applications of SBS in biomedical engineering are highlighted, showing enhanced cell infiltration and proliferation versus electrospun fiber scaffolds and in situ deposition of biodegradable polymers. We also discuss the impact of SBS in applications involving textiles and electronics, including ceramic fibers and conductive composite materials. Strategies for future research are presented that take advantage of direct and rapid polymer deposition via cost-effective methods.

Graphical abstract

[*]Corresponding Author: kofinas@umd.edu.

ORCID

John L. Daristotle: 0000-0002-3523-5390

Peter Kofinas: 0000-0001-6657-3037

Author Contributions

The manuscript was written through contributions of all authors. All authors have given approval to the final version of the manuscript.

Notes

The authors declare no competing financial interest.

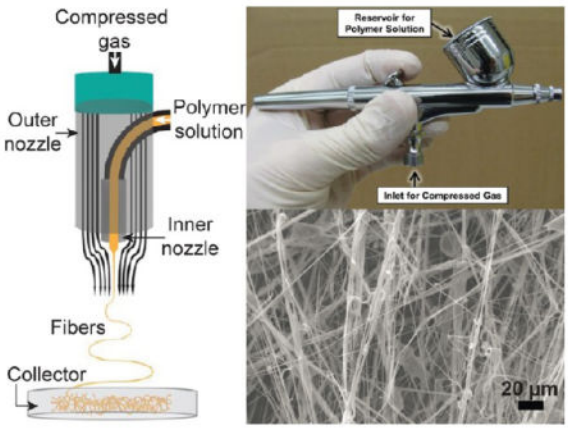

Keywords

solution blow spinning; nanofibers; nonwovens; fiber spinning; polymers; nanocomposites; microfibers

1. INTRODUCTION

Solution blow spinning (SBS) is a fiber fabrication process that requires two parallel concentric fluid streams: a polymer dissolved in a volatile solvent and a pressurized gas that flows around the polymer solution, creating fibers that are deposited in the direction of gas flow (Figure 1A). Generally, a SBS setup consists of a compressed gas source for delivering the carrier gas and a syringe pump for polymer solution (Figure 1B). The two streams can be easily integrated into a simple, easy-to-manufacture device (Figure 1C) or generated by using a commercially available airbrush (Figure 1D).[1,2] SBS also has the ability to deposit conformal fibers onto both planar and nonplanar substrates with a deposition rate that is approximately 10 times faster than conventional electrospinning.[2–4] The unique attributes of SBS provide a means to explore the utility of nonwoven fibrous materials in new fields. Such materials have been investigated for use in a wide variety of applications including electronics, filtration, and tissue engineering. New opportunities for applications include rapid biological scaffold generation and custom in situ materials fabrication.

In SBS, the carrier solvent evaporates quickly before the polymer fibers deposit on the collection surface. Although acute exposure to high concentrations of a solvent such as acetone may be toxic, studies have shown that SBS from acetone directly onto cells did not affect viability.[5] This allows SBS to be a biocompatible process. SBS does not require an electric field and uses a simple apparatus. The method is therefore easily implemented using inexpensive, transportable, and hand-held equipment.[2] When deployed as a technique to deposit materials in situ, SBS is capable of additive deposition of microfibers or nanofibers in custom conformal geometries.

In comparison to one of the most widely employed fiber fabrication techniques, electrospinning, SBS has fewer process requirements and variables. In electrospinning, polymers are commonly dissolved in highly toxic chlorinated or fluorinated solvents such as

dichloromethane, trifluoroethanol, or hexa-fluoro-2-propanol, which produce narrower, more consistent fibers because of their relatively high dielectric constants.[6,7] An additional limitation of electrospinning is that a large electric field must be applied to facilitate fiber production.[8] Fiber production is typically slow but well-controlled, precisely depositing a narrow distribution of fibers with solution deposition rates on the order of 1 mL hr^{-1}.[2] These factors limit both the commercial applicability of electrospun fibers and the capability of rapidly applying fibers for an immediate in situ indication.[9]

SBS uses processes similar to those used in industrial methods of fiber production, which enable its future applicability in large-scale production. For example, in a melt spinning or dry spinning process, a gas is used to cool or evaporate solvent from fibers, respectively, after extrusion through a spinneret by pumping. SBS uses a pressurized gas to both drive extrusion of the polymer solution *and* cause solvent evaporation, creating a polymer fiber in a simpler one-step process. Industrial production techniques allow for the continuous mass production of long fibers used in textile manufacturing applications. SBS allows for scalable production and deposition at the point and site of use. A compact deposition device can be easily manipulated by hand to deposit fibers in only the target area. Because the process is contained within the spinning device and the solvent evaporates within the working distance (typically 10–20 cm, but varies based on solvent volatility), polymer fibers are deposited with no further drying, cooling, or washing necessary.

Alternatives to electrospinning and common industrial spinning methods have been developed and characterized for specialty applications. These include techniques such as gas jet spinning, nozzle-free centrifugal spinning, rotary jet spinning, and flash-spinning.[10–14] Reviews on fiber spinning techniques have included brief introductions to SBS or similar techniques.[9,15] An increasing number of papers have been published on the subject (Figure 2), reflecting growing interest in this technology. Depending on the field, SBS research has been denoted “solution blowing” or “airbrushing”, but these techniques share the same governing principles. This review will compile research on techniques with similar principles, offering a comprehensive overview of SBS while highlighting recent applications and future value to researchers.

2. BASIC PRINCIPLES OF FIBER SPINNING

SBS fiber generation depends on the molecular weight of the polymer, concentration, and viscosity of the polymer solution, and process variables such as gas pressure and polymer solution flow rate. These parameters have direct influence on critical characteristics that enable the formation of a fiber-producing jet of polymer solution. The relationships between these variables and fiber morphology and diameter have been empirically and theoretically studied.

2.1. Theoretical Background and Modeling

The ability to form fibers from a jet of polymer solution is primarily governed by the entanglement of polymer chains. The overlap concentration (c^*) represents the critical point when polymer coils in solution begin to overlap, causing entanglements. When the overlap concentration is reached, a polymer solution becomes semidilute, and the interaction

between entangled polymer chains causes an increase in viscosity. c^* is best estimated by an equation for the semidilute, good solvent polymer environment:[16]

$$c^* = 6^{3/2} M_w / (8 N_a \langle R^2 \rangle^{3/2}) \quad (1)$$

An approximation of the mean-square end-to-end distance $\langle R^2 \rangle$ for the polymer–solvent system is necessary to calculate the overlap concentration required to form fibers (such as eq 2).[17]

$$\langle R^2 \rangle = \alpha^2 C_\infty \left(\frac{2M_w}{M_0} \right) l^2 \quad (2)$$

This can be found from the Flory expansion factor α, the characteristic ratio C_∞, and bond length l, which are used to represent deviations from ideality of polymer chain dimensions.[18] The weight-average molecular weight (M_w) of the polymer of interest and Avogadro's number (N_a) is also required.

Srinivasan et al. previously used the overlap concentration to explain fiber formation in an SBS process.[19] It has also been used to determine the onset of fiber formation in an electrospinning process, which shares the parameters of polymer concentration, polymer solution viscosity, and polymer solution flow rate but not electric field strength or electric field geometry.[20] The overlap concentration (c^*) represents the critical point when polymer entanglement becomes significant enough to stabilize the polymer jet, overcoming the inertio-capillary forces that drive bead formation instead of fiber formation under dilute conditions (Figure 3A). It has also been proposed that the entanglement concentration, $C_e \approx 10c^*$, approximates the concentration above which there will be no bead formation at all.[21]

The interplay between the viscous forces, inertio-capillary forces, and polymer relaxation time, which govern fiber formation of a polymer solution jet, can be represented by two dimensionless numbers: Deborah number (De, eq 3), and Ohnesorge number (Oh, eq 4).[22]

$$\mathrm{De} = \lambda / \sqrt{\rho r_0^3 / \sigma} \quad (3)$$

$$\mathrm{Oh} = \eta_0 / \sqrt{\rho \sigma r_0} \quad (4)$$

The exponential increase in zero-shear viscosity (η_0) caused by exceeding the overlap concentration causes viscous forces to dominate inertio-capillary forces, leading to fiber formation as observed in these studies. However, it is also evident from De that inertio-capillary forces must also be overcome in part by polymer relaxation time (λ), the time scale

for viscoelastic behavior of a polymer solution. λ increases proportionally to the entanglement of polymer chains and is insignificant for polymers with M_w less than the entanglement molecular weight, M_e.[23] This indicates that a polymer must have a minimum molecular weight, M_e, to make a solution capable of forming fibers. Inertio-capillary forces, represented by the denominator of both dimensionless numbers, can be altered by manipulating the solution density (ρ), solution surface tension (σ), and nozzle radius (r_0).

Investigations into the influence of molecular weight on fiber formation in fiber spinning process have yielded two additional insights: First, high-molecular-weight polymers can be spun into fibers at concentrations lower than their overlap concentration.[19] Srinivasan et al. confirmed the significance of De to fiber formation by estimating it for various polymer solutions over a range of polymer molecular weights and concentrations, all of which were at or below c^*. Despite Oh being similar for all solutions, increasing poly(methyl methacrylate) molecular weight produced increasing λ and therefore increasing De. This increase in polymer relaxation time coincided with the observation of increasingly fiber-like morphology, culminating with fiber formation at the highest molecular weight polymer solution, 2200 kDa, which possessed a concentration $c/c^* = 0.72$. Second, the extensibility average molecular weight (eq 5) can be used with the excluded volume constant ν to estimate a minimum spinning concentration for polymer blends (eq 6):[21]

$$M_L = \left(\frac{\sum_i N_i M_i^{2+\nu}}{\sum_i N_i M_i} \right)^{1/\nu+1} = \left(\sum_i w_i M_i^{1+\nu} \right)^{1/\nu+1} \quad (5)$$

$$c_{spin} \sim M_L^{-(\nu+1)} \quad (6)$$

SBS has been modeled as a Newtonian thin liquid jet moving in air.[24] Choosing a Newtonian model implies that the viscous forces dominate inertio-capillary forces (i.e., the polymer solution has a relatively high De). The fluid dynamics model described by Sinha-Ray et al. combines a series of mass and momentum balances on the straight and perturbed or “whipping” components of the jet to produce a time-dependent model of SBS jet dynamics. By accounting for the 3D position of the perturbed jet in turbulent flowing air, as well as concentration and viscosity changes due to solvent evaporation, this model is able to roughly estimate fiber size distribution and approximate the positioning of fibers deposited on a moving collector. The model moderately overestimates the fiber diameter distribution when compared to experimental data. Further investigating the role of local turbulence in fiber formation, Lou et al. developed a 2D computational fluid dynamics model to show the correlation of reliable fiber morphology with low turbulent intensity of the gas velocity field.[25] At gas pressures of 20 psi, a number approximating what is used in many SBS devices, peak turbulent intensity of the simulated flow field reached 35%. Experiments confirmed that at higher turbulent intensities, polymer jets had shorter straight segments, and fibers showed a wider diameter distribution. Their findings corroborate the frayed fiber morphology that has been observed by other groups at very high gas pressures (58 psi).[26] An

optimal gas pressure for consistent fiber formation is likely one that produces a flow field with velocities near the beginning of the turbulent regime.

These theoretical approaches indicate some of the critical parameters governing fiber formation by SBS. Overlap concentration and polymer relaxation time are key factors in polymer jet formation, implicating polymer concentration and molecular weight as key parameters governing process design. The polymer jet dynamics model indicates that polymer concentration, polymer flow rate, air flow rate, and nozzle dimensions will affect fiber diameter. The theoretical importance of variables such as polymer concentration and air flow rate justify the empirical approaches used by many groups to correlate critical parameters with fiber mat morphologies. These empirical approaches will be reviewed in the next section.

2.2. Empirical Studies

2.2.1. Polymer Concentration and Molecular Weight—Multiple studies have examined the effects of polymer molecular weight or polymer concentration on fiber formation and morphology. Confirming the critical role that overlap concentration eq 1 plays in enabling fiber formation, experiments have confirmed that SBS forms fibers above c^* ($c > c^*$), "beads-on-a-string" near c^* ($c \sim c^*$), and corpuscular morphologies below c^* ($c < c^*$).[19] Both poly(methyl methacrylate) molecular weight and concentration were varied across a range spanning the estimated overlap concentration (using eq 1 and parameters from the literature) to visualize morphological changes under scanning electron microscopy (SEM) (Figure 3B). Increasing concentration also produced a beads-on-a-string to fiber morphological transition with poly-(lactic-*co*-glycolic acid) (PLGA).[5]

Furthermore, within the domain $c > c^*$, empirical studies show that fiber diameter increases with increasing concentration. For poly(lactic acid) (PLA) fibers produced via SBS, increasing polymer concentration from 4% w/v to 8% w/v produced fiber distributions with a greater average diameter.[26] This trend was confirmed with poly(ethylene oxide) (PEO) in a separate study.[25] However, increasing gas pressure reduced the effect of increased concentration.[26] The effects of gas pressure will be covered in depth in the next section.

2.2.2. Process Variables—Fiber diameter is only affected by polymer solution flow rate at low gas pressures.[26] However, low and high feed rates may cause jet instability and nozzle clogging, respectively. Useable feed rates vary based on SBS device but generally range from 0.02 to 1 mL min $^{-1}$.[2,4,26] Observations of nozzle clogging and jet instability at suboptimal operating conditions have been reported by multiple research groups.[2,5,26,27] Decreasing nozzle diameter decreases fiber diameter.[25] Increasing gas pressure produces a narrower fiber diameter distribution with less variance and consistent fiber morphology, which is preferred for applications that require precise fiber diameter (Figure 4A–C).[5,26,28] However, increasing gas flow rate beyond the optimal range may also cause a temperature decrease at the SBS device due to gas expansion, which decreases temperature proportional to the volumetric expansion of the carrier gas.[5] This may cause poor solvent evaporation and fiber welding (Figure 4C). The observation of a stable polymer jet has led researchers to search for an optimal set of polymer flow rates and air pressures. Most blow spinning

devices operate with polymer streams at room temperature, however, temperature of the polymer stream may be increased to reduce the viscosity of the polymer solution or increase solubility of the polymer.[29]

2.3. Choice of Polymer–Solvent System

Using information from the previous section, we propose a set of general rules to guide polymer and solvent selection for SBS of polymer fibers. The chosen solvent must be a good solvent for the polymer to be dissolved up to at least c^*. The concentration of the polymer in solution must be greater than c^* to enable fiber formation, and potentially higher to completely eliminate bead formation. Lastly, the polymer molecular weight must be high enough to create entanglements between polymer chains, producing a sufficiently high polymer relaxation time. Satisfying these minimum criteria will ensure the production of polymer fibers. When using a solvent with exceptionally high or low inherent surface tension, such as water, it may also be necessary to consider the contribution of surface tension to the capillary forces that oppose fiber formation. It may be viable to increase solvent evaporation by controlling the temperature and humidity of the surrounding environment during SBS, or using a large working distance (50 cm).[25,29] Solvent quality and evaporation rate may also affect the crystallinity of the fibers formed by SBS.[30] Filler content, such as nanoparticles, can increase the viscosity of a polymer solution and therefore will affect the morphology of fibers as described in the previous sections.[31] This has also been demonstrated in previous studies of electrospun composite fibers, which showed that fillers can be used to modulate the viscosity of polymer solutions, but fiber formation is still controlled by meeting the minimum polymer concentration requirement of c^*.[32]

3. STRUCTURE AND PROPERTIES OF FIBERS

3.1. Morphology

Controlling the microstructure, morphology, and alignment of fibers enables the fabrication of multifunctional fibrous materials, including fibrous composites, tissue engineering scaffolds with enhanced regenerative potential, and nonwoven textiles with increased surface area and desirable transport properties.[33–36] To address these needs, SBS has been used to easily create fibers conferred with unique morphologies, various microstructural features, and diverse mechanical properties. Fibers with diameters ranging from ~100 nm to greater than 1 μm have been fabricated by SBS. Aligned fiber mats can be created by spinning onto a rolling collector, similar to meltspinning and electrospinning.[3] By modulating the concentration of polymer in the polymer solution, SBS can be used to produce polymer constructs with fibrous, beads on a string, and corpuscular morphologies for enhanced surface properties, such as increased omniphobicity.[19] Porosity and fiber branching can be controlled using process variables such as polymer concentration and polymer blending.[26,37]

SBS and electrospinning produce fiber mats with different morphological characteristics. Overall porosity (77–95%) and pore size (8–17 μm) of SBS scaffolds are greater than those of scaffolds produced by electrospinning with similar polymers (67% and 3 μm, respectively).[2] Tutak et al. demonstrated that SBS may produce fiber bundles, a nonuniform morphology not associated with electrospinning (Figure 5A, B). This observation was

confirmed by Bolbasov et al. using polyvinylidene fluoride-trifluoroethylene copolymer (VDF-TeFE).[38] Tutak et al. also observed that SBS produces fibers with a tighter diameter distribution than electrospinning, an observation that was confirmed by Oliveira et al.[39] Locally nonuniform structural control may provide a means to investigate cell response to specific three-dimensional biomimetic structures, such as aligned fibrils, which have been shown to modulate cell migration and protein expression in collagen matrices.[40] To further increase scaffold porosity and enhance cell infiltration, Medeiros et al. recently developed cryogenic SBS.[41] This technique simultaneously incorporates ice spheres into freeze-dried fibers, creating macroporous fibers when the scaffold is deployed and the ice melts.

3.2. Mechanical Properties

The mechanical properties of a fiber scaffold can be critical to its end use (e.g. as a nonwoven textile, or a feature used to increase effectiveness, such as in cell infiltration). Young's modulus, failure strain, and failure stress, derived from a stress–strain curve, are frequently reported for materials of interest. However, few studies have comprehensively examined the mechanical properties of SBS fiber scaffolds. One study has compared the mechanical properties of polycaprolactone (PCL) scaffolds produced by SBS and electrospinning, and the investigators found that electrospinning produced fiber mats with approximately 10 times higher Young's modulus (Figure 5C, D).[2] SEMs showed greater fiber entanglement in the electrospun scaffolds, which likely caused them to have greater stiffness (Figure 5A, B). Another compared the mechanical properties of VDF-TeFE copolymers fabricated by SBS and electrospinning.[38] SBS again produced mats with local fiber bundles, unlike electrospinning, and lower tensile strength. Electrospinning processes can also be tuned to align and organize fibers using additional equipment, such as rotating collectors or counter electrodes, allowing an electrospinning setup to produce similar local orientation or levels of entanglement.[42–45] Block copolymer fiber mats fabricated by SBS have demonstrated notable elasticity and strain recovery (Figure 5E).[1] Energy dissipation studies showed the modes of failure for fiber mats produced by SBS, which are fiber rearrangement, broken fiber connections, and individual fiber deformation.[1] Further investigation is required into the connection between the bundled morphology of SBS fiber mats and their mechanical properties. Fiber bundles may be related to turbulent air flow around the polymer jet and subsequent bending instability, which causes multiple streams of solution to emerge from a single nozzle (Figure 6A). Multiple fibers may be formed simultaneously and thus deposited in the same area with alignment. Lower gas pressures may reduce these instabilities (Figure 6B, C).[46] Fiber mats with lower modulus may better approximate the mechanical properties of soft biological materials such as fibrin (1–10 MPa) or human skin (0.1–1 MPa).[47,48]

3.3. Multicomponent Polymer Fibers

Multicomponent polymer mixtures and coaxial SBS setups with concentric nozzles have been used to create polymer fibers with well-defined heterogeneous polymer distributions. Oliveira et al. used a blend of PEO and PLA to fabricate fibers with a core of amorphous PLA and shell of semicrystalline PEO when blended at a 1:1 ratio (Figure 7A).[49] Core–shell amorphous polymer fibers have been created from coaxial SBS of poly(methyl methacrylate) (PMMA) and polyacrylonitrile (PAN), soy protein and nylon-6, and wood

cellulose pulp and PEO.[50–52] In the last two examples, the polymer shell was employed to stabilize the formation of the fiber core, which could not be formed alone. Core–shell fibers with epoxy precursors or other self-healing monomers loaded in the core exhibited self-healing properties and increased fatigue strength.[53–55]

Polymer blends have also been used with SBS to tailor the properties of homogeneous polymer fibers. Liu et al. blended chitosan and poly(vinyl alcohol) (PVA) with varying amounts of cross-linker to create swellable hydrogel nanofibers (Figure 7B, C).[56] Behrens et al. blended PLGA and poly(ethylene glycol) (PEG) in various compositions to tune the glass transition temperature of polymer fibers, though this also affected the fiber diameter and morphology (Figure 7D–F).[57] PEG content also modulates swelling and permeability in chitosan/PLA blend fibers.[58] Polymer blending using polymers of different molecular weights can alter degradation rate.[37] Mixtures of polymer with nonpolymer additives such as zirconium-modified amorphous calcium phosphate and low-surface-energy cage molecule 1*H*,1*H*,2*H*,2*H*-heptadecafluorodecyl polyhedral oligomeric silsesquioxane have been used to tailor surface properties of fibers made by SBS.[19,59] Research groups have also used SBS to airbrush fibers with liquid crystal cores and polymer shells formed through spontaneous phase separation during the spraying process.[60]

4. SBS APPLICATIONS AND INNOVATIONS

SBS allows for portable, conformal fiber deposition on any substrate. This dramatically expands the number of possible applications for nanofiber-based technologies. Previously, possible targets for fiber deposition were limited by restraints inherent to the technique: electrospinning requires an applied voltage and conductive target, while industrial processes require cumbersome equipment. As a result, the most impactful research using SBS has studied direct deposition onto the target of interest, especially on biological substrates. The following discussion will highlight these applications, how each application has improved upon or integrated conventional techniques in its field, and the broader significance and future impact that we project each application will have.

4.1. Biomedical Applications of Polymer Fibers

Polymer fiber mats produced by SBS are porous, making them ideal for use as a cell scaffold. Fibrous scaffolds are designed to foster cell proliferation, differentiation, and infiltration. SBS can produce nanofiber scaffolds capable of culturing human bone marrow stromal cells (hBMSCs).[2] The porosity and pore size of SBS scaffolds facilitate cell infiltration. A direct comparison of hBMSCs cultured on blow spun and electrospun scaffolds showed that hBMSCs cultured on blow spun scaffolds penetrated 78.75 ± 18.46 μm, significantly deeper than on electrospun scaffolds (34.75 ± 8.77 μm).[59] Mesenchymal stem cell (MSC) proliferation and differentiation was also measured on VDF-TeFE scaffolds produced by SBS and electrospinning.[38] MSCs differentiated into a higher fraction of proliferative phenotype when cultured on SBS scaffolds and produced more total cells (Figure 8A–C). Polymer nanofiber scaffolds were shown to increase cellular peroxidase activity and influence organelle positioning versus polymer films of the same composition.[61] SBS has also been used to fabricate PLA implants loaded with dibasic calcium phosphate

dehydrate filler.[62] These implants were shown to be oncologically safe as they do not stimulate the growth of tumors adjacent to the implant.

Tissue engineering and regenerative medicine will benefit from the versatility of conformal deposition by SBS. Target wounds and defects for tissue replacement have varying size and geometry, making adaptable materials fabrication a necessity for the clinical future of these fields. Furthermore, as a field, tissue engineering has devoted significant resources to developing custom materials fabrications systems, such as 3D printers and injectable hydrogels.[63] SBS can meet a subset of these needs by providing timely, on-demand polymer fiber deposition.[5] SBS is also compatible with a variety of additives that have been shown to enhance regenerative potential, such as osteogenic zirconium-modified amorphous calcium phosphate.[59] Nanoparticles of bioactive glass have also been used as additive in SBS scaffolds and delivered using a burst release.[41] Solvent toxicity is a problem with electrospun fiber scaffolds that has been addressed by melt-electrospinning processes, which spin polymer melts to avoid the need for solvent.[64] SBS inherently solves this problem by volatilizing the spinning solvent: acetone showed no cytotoxicity when sprayed at a distance of 10 cm directly onto cell culture plates, both during fiber deposition and alone.[5] SBS can be performed aseptically in a sterile environment.[65]

Medical applications are uniquely suited for direct fiber deposition in targets and will also be able to utilize the properties of SBS that make it particularly biocompatible: low toxicity, high porosity, and compatibility with biodegradable materials. SBS has been used to directly coat medical devices with lubricant-infused poly(styrene-*b*-isobutylene-*b*-styrene) (SIBS) microfibers, which can resist thrombosis and bacterial attachment with low cytotoxicity.[66] The addition of silicon oil prevented the adhesion of blood cells (Figure 8D, E). Some promising biodegradable and absorbable polymers previously used in U.S. Food and Drug Administration-approved products have been used with SBS (Table 1). An initial investigation of PLGA fibers for biomedical applications demonstrated nontoxicity of the SBS process, hydrolytic degradation of the fibers leading to morphological changes, interactions between nanofibers and blood, and in situ deposition in porcine models of lung resection, intestinal anastomosis, liver injury, and diaphragmatic hernia.[5] In situ conformal deposition by SBS from a commercial airbrush allowed for complete coverage of tissues with polymer fibers (Figure 8F), which transitioned to an adhesive film for use as a surgical sealant (Figure 8G).[57] Polymer fibers have also been created with SBS for antibacterial activity using biopolymers, PLA/polyvinylpyrrolidone (PVP) blends, and chitosan/PLA/PEG blends loaded with antibacterial additives.[56,67,68] Controlled drug delivery has been achieved using nanostructured membranes and core–shell fibers.[69,70] Desorption was determined to be the limiting factor in release of a hydrophobic drug, and poragens such as PEG were used to control release rate.[71] An electrochemical glucose biosensor and metal ion sensor for potable water were also developed based on a platform of fibers spun from a mixture of PLA and carbon.[72,73]

4.2. Polymer Fibers for Coatings, Textiles, and Electronics

SBS has its conceptual roots in fiber spinning techniques that are commonly used in industrial fiber production processes, such as polymer solution spinning from a spinneret to

create textiles.[74] Many of the same physical principles govern both processes. Due to its simplicity and ability to directly deliver conformal fibers, it has been investigated for creating functional polymer nanofiber coatings, nonwoven textiles, and stretchable electronics. These investigations have shown that SBS can produce fibrous materials with high precision, efficiency, and reliability.

Fibrous coatings may utilize porous microstructures with re-entrant surface features to maximize omniphobicity.[75] SBS can produce superomniphobic fibrous coatings with finely tuned corpuscular microstructure controlled by polymer concentration in solution, with the eventual possibility of direct, conformal delivery.[19] It proved to be an efficient method for nanofiber generation, safely, and cost-effectively delivering nanofibers at high deposition rates with the potential for further process scaling.[2,4] SBS has also been used for filter and membrane applications. Shi et al. prepared air filters from nylon-6, and Lee et al. prepared water purification membranes from nylon-6 fibers entangled with graphene flakes during the spraying process.[76,77] PAN-based activated carbon fibers were fabricated with SBS and used for CO_2 adsorption and phenol adsorption.[78,79] Ultrafine 20–50 nm fibers produced by SBS can be used for nanoparticle filtration.[80] Poly(ether sulfone)/Nafion and poly(ether ether ketone)/Nafion composite proton exchange membranes were also fabricated using SBS fibers impregnated with Nafion solution.[81–83]

SBS has been used to fabricate stretchable conductive materials, via silver nanoparticle-based solution-processing techniques.[1] By conformally depositing this material on a hand and measuring electronic resistance (Figure 9A), this research shows the potential of using SBS to develop wearable smart materials. Fibrous composite electronic devices show enhanced stretchability and conductivity. SBS enables their deposition on nonplanar substrates, which has the potential to enhance commercial applicability. SBS can also serve as the framework for advanced processing methods, such as carbon nanofiber production (Figure 9B–C).[51,84] Similarly, yarns of carbon nanofibers were produced using PAN as a precursor polymer.[85] By spinning onto two rods, a yarn was formed. SBS fiber mats have also been used as a precursor for alumina, zirconia, and mullite fiber preparation.[86–88] Y–Ba–Cu–O oxide ceramic fibers were fabricated for use in superconducting applications.[89] Ceramic nanofibers of TiO_2 and ZnO with high surface area have been fabricated using SBS from a mixture of Ti or Zn sources and polymer in solution, followed by postprocessing.[90] The primary advantage of using SBS to fabricate these materials is increased production rate, which will make processes more cost-efficient and thus more accessible to researchers and markets. Depending on the type of ceramic fiber, production rates typically increase by a factor of 5–10 when using SBS compared to conventional electrospinning.[89,91]

5. FUTURE DIRECTIONS

SBS provides opportunities for expanding upon the foundation of nanofiber-based research investigated in the literature using the electrospinning technique. SBS has fewer constraints than electrospinning. Because fiber formation is not driven by an electric field, there is no effect on fiber diameter from the electrical conductivity of the polymer solution and, subsequently, no incentive to use highly toxic fluorinated solvents. Furthermore, the simple apparatus required for SBS will allow researchers to investigate new applications for

nanofibrous and microfbrous materials. Because they can be deposited on demand, SBS can feasibly create conformal coatings, textiles, and materials with custom geometries from a scalable self-contained process. This is a necessary innovation for the advancement of fields such as wearable electronics and healthcare materials.[92,93]

Direct deposition onto living targets requires further investigation as a method for creating biological scaffolds, especially given the differences in fiber morphology observed between electrospinning and SBS. Previous research has demonstrated the viability of cells deposited from an air-brush.[94,95] Crucial parameters such as polymer concentration, solution viscosity, and spraying technique may affect cell viability but do not prevent the simultaneous deposition of cells and material.[96] Biological materials, such as collagen and silk, merit further investigation as a material source for SBS given their outstanding mechanical properties, particularly if they can be spun in their native folded state and then used to fabricate low-cost biomimetic materials.[97] A number of biological materials have been spun into fibers by SBS, including soy protein, fish sarcoplasmic protein, and cellulose acetate (Table 2).[52,98,99] In conjunction, novel modifications to the general SBS technique can allow for spinning from new solvents, such as water or dimethyl carbonate, and the ability to deposit cells (Figure 10A, B).[29,65,100]

SBS will enable researchers to develop materials that are translatable to commercial markets. Scalability and safety are necessary for the widespread applicability of nanofibrous materials.[9] Beyond simple advantages in portability due to the fact that SBS can deposit fibers onto any target, SBS is a more cost-effective and rapid technique for generating nanofibers than electrospinning.[2] Costs are minimized when a gravity-fed or siphon-fed airbrush is used, while deposition rates are on the order of 10 times faster than electrospinning. Various research groups have increased process scale by using multiple nozzles[27,101] and grids[65] (Figure 10C). Mahalingam et al. complexed SBS with centrifugal spinning to increase production.[102] Safety concerns related to the usage of toxic solvents can also be minimized by using volatile solvents with limited toxicity that evaporate before accumulating at the surface of the fiber collector. SBS is also adaptable to spinning many different types of polymer-composite and polymer-composite precursor mixtures (Table 3). This enables the costeffective fabrication of highly functional nonwoven nanotextiles, which may have increased durability or provide optical responses to external stimuli.[103]

Further research into the fundamental parameters governing SBS fiber formation is required. It is clear that a multitude of factors such as polymer concentration and gas pressure influence fiber diameter and morphology, but the effects of solvent evaporation rate, polymer molecular weight, polymer blends and solution additives, and nozzle type require further investigation. It is also important to clarify the differences between variations of the SBS technique.[104] Research on well-studied fiber spinning techniques similar to SBS may provide insight on how to answer these questions.[9]

6. CONCLUSIONS

SBS is a fabrication technique that enables on-demand, in situ fiber generation using a simple apparatus. Theoretical and empirical models of fiber production using this technique

have revealed basic relationships between polymer solution concentration, gas pressure, and fiber diameter. These studies also emphasize the importance of overlap concentration and molecular weight in determining the spinnability of a polymer solution. SBS materials have a bundled morphology and unique mechanical properties. Special techniques and multicomponent blends can be used to produce functional architectures, such as core–shell fibers. A range of applications involving polymer nanofibers generated by SBS in biomaterials, tissue engineering, textiles, and composites have been highlighted. In the future, SBS will be most valuable to the research community as an avenue for exploring new combinations of polymers and solvents not accessible to electrospinning, and as a technique for conveniently producing translatable fibrous materials.

Acknowledgments

Research reported in this publication was supported by the National Institute of Biomedical Imaging and Bioengineering of the National Institutes of Health under Award No. R01EB019963. The content is solely the responsibility of the authors and does not necessarily represent the official views of the National Institutes of Health. The authors would like to thank Dr. Omar Ayyub for helpful discussions.

References

1. Vural M, Behrens AM, Ayyub OB, Ayoub JJ, Kofinas P. Sprayable Elastic Conductors Based on Block Copolymer Silver Nanoparticle Composites. ACS Nano. 2015; 9(1):336–344. [PubMed: 25491507]
2. Tutak W, Sarkar S, Lin-Gibson S, Farooque TM, Jyotsnendu G, Wang D, Kohn J, Bolikal D, Simon CG. The Support of Bone Marrow Stromal Cell Differentiation by Airbrushed Nanofiber Scaffolds. Biomaterials. 2013; 34(10):2389–2398. [PubMed: 23312903]
3. Medeiros ES, Glenn GM, Klamczynski AP, Orts WJ, Mattoso LHC. Solution Blow Spinning: A New Method to Produce Micro- and Nanofibers from Polymer Solutions. J Appl Polym Sci. 2009; 113(4):2322–2330.
4. Polat Y, Pampal ES, Stojanovska E, Simsek R, Hassanin A, Kilic A, Demir A, Yilmaz S. Solution Blowing of Thermoplastic Polyurethane Nanofibers: A Facile Method to Produce Flexible Porous Materials. J Appl Polym Sci. 2016; 133(9):43025.
5. Behrens AM, Casey BJ, Sikorski MJ, Wu KL, Tutak W, Sandler AD, Kofinas P. In Situ Deposition of PLGA Nanofibers via Solution Blow Spinning. ACS Macro Lett. 2014; 3(3):249–254.
6. Son WK, Youk JH, Lee TS, Park WH. The Effects of Solution Properties and Polyelectrolyte on Electrospinning of Ultrafine Poly(ethylene Oxide) Fibers. Polymer. 2004; 45(9):2959–2966.
7. Luo CJ, Nangrejo M, Edirisinghe M. A Novel Method of Selecting Solvents for Polymer Electrospinning. Polymer. 2010; 51(7):1654–1662.
8. Greiner A, Wendorff JH. Electrospinning: A Fascinating Method for the Preparation of Ultrathin Fibers. Angew Chem, Int Ed. 2007; 46(30):5670–5703.
9. Luo CJ, Stoyanov SD, Stride E, Pelan E, Edirisinghe M. Electrospinning versus Fibre Production Methods: From Specifics to Technological Convergence. Chem Soc Rev. 2012; 41(13):4708–4735. [PubMed: 22618026]
10. Badrossamay MR, McIlwee HA, Goss JA, Parker KK. Nanofiber Assembly by Rotary Jet-Spinning. Nano Lett. 2010; 10(6):2257–2261. [PubMed: 20491499]
11. Benavides RE, Jana SC, Reneker DH. Nanofibers from Scalable Gas Jet Process. ACS Macro Lett. 2012; 1(8):1032–1036.
12. Weitz RT, Harnau L, Rauschenbach S, Burghard M, Kern K. Polymer Nanofibers via Nozzle-Free Centrifugal Spinning. Nano Lett. 2008; 8(4):1187–1191. [PubMed: 18307320]
13. Dean, AR., Emilio, RJ. Process and Apparatus for Flash Spinning of Fibrillated Plexifilamentary Material. US Patent. US3227794 A. Jan 4. 1966

14. Kim SY, Purnama P, Kim SH. Fabrication of Poly(l-Lactide) Fibers/sheets Using Supercritical Fluid through Flash-Spinning Process. Macromol Res. 2010; 18(12):1233–1236.
15. Stojanovska E, Canbay E, Pampal ES, Calisir MD, Agma O, Polat Y, Simsek R, Gundogdu NAS, Akgul Y, Kilic A. A Review on Non-Electro Nanofibre Spinning Techniques. RSC Adv. 2016; 6(87):83783–83801.
16. Graessley WW. Polymer Chain Dimensions and the Dependence of Viscoelastic Properties on Concentration, Molecular Weight and Solvent Power. Polymer. 1980; 21(3):258–262.
17. Flory, PJ. Statistical Mechanics of Chain Molecules. Interscience Publishers; Geneva, Switzerland: 1969.
18. Flory, PJ. Principles of Polymer Chemistry. Cornell University Press; Ithaca, NY: 1953.
19. Srinivasan S, Chhatre SS, Mabry JM, Cohen RE, McKinley GH. Solution Spraying of Poly(methyl Methacrylate) Blends to Fabricate Microtextured, Superoleophobic Surfaces. Polymer. 2011; 52(14):3209–3218.
20. Shenoy SL, Bates WD, Frisch HL, Wnek GE. Role of Chain Entanglements on Fiber Formation during Electrospinning of Polymer Solutions: Good Solvent, Non-Specific Polymer–polymer Interaction Limit. Polymer. 2005; 46(10):3372–3384.
21. Palangetic L, Reddy NK, Srinivasan S, Cohen RE, McKinley GH, Clasen C. Dispersity and Spinnability: Why Highly Polydisperse Polymer Solutions Are Desirable for Electrospinning. Polymer. 2014; 55(19):4920–4931.
22. McKinley GH. Dimensionless Groups for Understanding Free Surface Flows of Complex Fluids. Soc Rheol Bull. 2005; 2005:6–9.
23. Graessley, WW. Advances in Polymer Science. Vol. 16. Springer; Berlin Heidelberg: 1974. The Entanglement Concept in Polymer Rheology.
24. Sinha-Ray S, Sinha-Ray S, Yarin AL, Pourdeyhimi B. Theoretical and Experimental Investigation of Physical Mechanisms Responsible for Polymer Nanofiber Formation in Solution Blowing. Polymer. 2015; 56:452–463.
25. Lou H, Li W, Li C, Wang X. Systematic Investigation on Parameters of Solution Blown Micro/nanofibers Using Response Surface Methodology Based on Box-Behnken Design. J Appl Polym Sci. 2013; 130(2):1383–1391.
26. Oliveira JE, Moraes EA, Costa RGF, Afonso AS, Mattoso LHC, Orts WJ, Medeiros ES. Nano and Submicrometric Fibers of poly(D,L-Lactide) Obtained by Solution Blow Spinning: Process and Solution Variables. J Appl Polym Sci. 2011; 122(5):3396–3405.
27. Kolbasov A, Sinha-Ray S, Joijode A, Hassan MA, Brown D, Maze B, Pourdeyhimi B, Yarin AL. Industrial-Scale Solution Blowing of Soy Protein Nanofibers. Ind Eng Chem Res. 2016; 55(1): 323–333.
28. Zhang L, Kopperstad P, West M, Hedin N, Fong H. Generation of Polymer Ultrafine Fibers through Solution (Air-) Blowing. J Appl Polym Sci. 2009; 114(6):3479–3486.
29. Santos AMC, Medeiros ELG, Blaker JJ, Medeiros ES. Aqueous Solution Blow Spinning of Poly(vinyl Alcohol) Micro- and Nanofibers. Mater Lett. 2016; 176:122–126.
30. Oliveira J, Brichi GS, Marconcini JM, Mattoso LHC, Glenn GM, Medeiros ES. Effect of Solvent on the Physical and Morphological Properties of Poly (Lactic Acid) Nanofibers Obtained by Solution Blow Spinning. J Eng Fibers Fabr. 2014; 9(4):117–125.
31. Nicodemo L, Nicolais L. Viscosity of Bead Suspensions in Polymeric Solutions. J Appl Polym Sci. 1974; 18(9):2809–2818.
32. Drew C, Wang X, Samuelson LA, Kumar J. The Effect of Viscosity and Filler on Electrospun Fiber Morphology. J Macromol Sci, Part A: Pure Appl Chem. 2003; 40(12):1415–1422.
33. Baji A, Mai Y-W, Wong S-C, Abtahi M, Chen P. Electrospinning of Polymer Nanofibers: Effects on Oriented Morphology, Structures and Tensile Properties. Compos Sci Technol. 2010; 70(5): 703–718.
34. Baker BM, Mauck RL. The Effect of Nanofiber Alignment on the Maturation of Engineered Meniscus Constructs. Biomaterials. 2007; 28(11):1967–1977. [PubMed: 17250888]
35. Deitzel JM, Kleinmeyer J, Harris DEA, Beck Tan NC. The Effect of Processing Variables on the Morphology of Electrospun Nanofibers and Textiles. Polymer. 2001; 42(1):261–272.

36. Gibson P, Schreuder-Gibson H, Rivin D. Transport Properties of Porous Membranes Based on Electrospun Nanofibers. Colloids Surf, A. 2001; 187–188:469–481.
37. Behrens AM, Kim J, Hotaling N, Seppala JE, Kofinas P, Tutak W. Rapid Fabrication of poly(DL-Lactide) Nanofiber Scaffolds with Tunable Degradation for Tissue Engineering Applications by Air-Brushing. Biomed Mater. 2016; 11(3):035001. [PubMed: 27121660]
38. Bolbasov EN, Stankevich KS, Sudarev EA, Bouznik VM, Kudryavtseva VL, Antonova LV, Matveeva VG, Anissimov YG, Tverdokhlebov SI. The Investigation of the Production Method Influence on the Structure and Properties of the Ferroelectric Nonwoven Materials Based on Vinylidene Fluoride – Tetrafluoro-ethylene Copolymer. Mater Chem Phys. 2016; 182:338–346.
39. Oliveira JE, Mattoso LH, Orts WJ, Medeiros ES. Structural and Morphological Characterization of Micro and Nanofibers Produced by Electrospinning and Solution Blow Spinning: A Comparative Study. Adv Mater Sci Eng. 2013; 2013:409572.
40. Fraley SI, Wu P, He L, Feng Y, Krisnamurthy R, Longmore GD, Wirtz D. Three-Dimensional Matrix Fiber Alignment Modulates Cell Migration and MT1-MMP Utility by Spatially and Temporally Directing Protrusions. Sci Rep. 2015; 5:14580. [PubMed: 26423227]
41. Medeiros ELG, Braz AL, Porto IJ, Menner A, Bismarck A, Boccaccini AR, Lepry WC, Nazhat SN, Medeiros ES, Blaker JJ. Porous Bioactive Nanofibers via Cryogenic Solution Blow Spinning and Their Formation into 3D Macroporous Scaffolds. ACS Biomater Sci Eng. 2016; 2(9):1442–1449.
42. Bhattarai N, Edmondson D, Veiseh O, Matsen FA, Zhang M. Electrospun Chitosan-Based Nanofibers and Their Cellular Compatibility. Biomaterials. 2005; 26(31):6176–6184. [PubMed: 15885770]
43. Teo WE, Ramakrishna S. A Review on Electrospinning Design and Nanofibre Assemblies. Nanotechnology. 2006; 17(14):R89–R106. [PubMed: 19661572]
44. Wu H, Zhang R, Liu X, Lin D, Pan W. Electrospinning of Fe, Co, and Ni Nanofibers: Synthesis, Assembly, and Magnetic Properties. Chem Mater. 2007; 19(14):3506–3511.
45. Li D, Wang Y, Xia Y. Electrospinning of Polymeric and Ceramic Nanofibers as Uniaxially Aligned Arrays. Nano Lett. 2003; 3(8):1167–1171.
46. Lou H, Han W, Wang X. Numerical Study on the Solution Blowing Annular Jet and Its Correlation with Fiber Morphology. Ind Eng Chem Res. 2014; 53(7):2830–2838.
47. Collet J-P, Shuman H, Ledger RE, Lee S, Weisel JW. The Elasticity of an Individual Fibrin Fiber in a Clot. Proc Natl Acad Sci U S A. 2005; 102(26):9133–9137. [PubMed: 15967976]
48. Agache PG, Monneur C, Leveque JL, De Rigal J. Mechanical Properties and Young's Modulus of Human Skin in Vivo. Arch Dermatol Res. 1980; 269(3):221–232. [PubMed: 7235730]
49. Oliveira JE, Moraes EA, Marconcini JM, Mattoso LHC, Glenn GM, Medeiros ES. Properties of Poly(lactic Acid) and Poly(ethylene Oxide) Solvent Polymer Mixtures and Nanofibers Made by Solution Blow Spinning. J Appl Polym Sci. 2013; 129(6):3672–3681.
50. Zhuang X, Yang X, Shi L, Cheng B, Guan K, Kang W. Solution Blowing of Submicron-Scale Cellulose Fibers. Carbohydr Polym. 2012; 90(2):982–987. [PubMed: 22840029]
51. Sinha-Ray S, Yarin AL, Pourdeyhimi B. The Production of 100/400 Nm Inner/outer Diameter Carbon Tubes by Solution Blowing and Carbonization of Core–shell Nanofibers. Carbon. 2010; 48(12):3575–3578.
52. Sinha-Ray S, Zhang Y, Yarin AL, Davis SC, Pourdeyhimi B. Solution Blowing of Soy Protein Fibers. Biomacromolecules. 2011; 12(6):2357–2363. [PubMed: 21553861]
53. Lee MW, Yoon SS, Yarin AL. Solution-Blown Core–Shell Self-Healing Nano- and Microfibers. ACS Appl Mater Interfaces. 2016; 8(7):4955–4962. [PubMed: 26836581]
54. Lee MW, Sett S, Yoon SS, Yarin AL. Fatigue of Self-Healing Nanofiber-Based Composites: Static Test and Subcritical Crack Propagation. ACS Appl Mater Interfaces. 2016; 8(28):18462–18470. [PubMed: 27332924]
55. Sinha-Ray S, Pelot DD, Zhou ZP, Rahman A, Wu X-F, Yarin AL. Encapsulation of Self-Healing Materials by Coelectrospinning, Emulsion Electrospinning, Solution Blowing and Intercalation. J Mater Chem. 2012; 22(18):9138–9146.
56. Liu R, Xu X, Zhuang X, Cheng B. Solution Blowing of chitosan/PVA Hydrogel Nanofiber Mats. Carbohydr Polym. 2014; 101:1116–1121. [PubMed: 24299882]

57. Behrens AM, Lee NG, Casey BJ, Srinivasan P, Sikorski MJ, Daristotle JL, Sandler AD, Kofinas P. Biodegradable-Polymer-Blend-Based Surgical Sealant with Body-Temperature-Mediated Adhesion. Adv Mater. 2015; 27(48):8056–8061. [PubMed: 26554545]
58. Xu X, Zhou G, Li X, Zhuang X, Wang W, Cai Z, Li M, Li H. Solution Blowing of chitosan/PLA/PEG Hydrogel Nanofibers for Wound Dressing. Fibers Polym. 2016; 17(2):205–211.
59. Hoffman K, Skrtic D, Sun J, Tutak W. Airbrushed Composite Polymer Zr-ACP Nanofiber Scaffolds with Improved Cell Penetration for Bone Tissue Regeneration. Tissue Eng, Part C. 2015; 21(3):284–291.
60. Wang J, Jákli A, West JL. Airbrush Formation of Liquid Crystal/Polymer Fibers. Chem Phys Chem. 2015; 16(9):1839–1841. [PubMed: 25823369]
61. Tutak W, Jyotsnendu G, Bajcsy P, Simon CG. Nanofiber Scaffolds Influence Organelle Structure and Function in Bone Marrow Stromal Cells. J Biomed Mater Res, Part B. 2016; [Online early access]. doi: 10.1002/jbm.b.33624
62. Litviakov NV, Tverdokhlebov SI, Perelmuter VM, Kulbakin DE, Bolbasov EN, Tsyganov MM, Zheravin AA, Svetlichnyi VA, Cherdyntseva NV. AIP Conf Proc. 2016:020043.
63. Billiet T, Vandenhaute M, Schelfhout J, Van Vlierberghe S, Dubruel P. A Review of Trends and Limitations in Hydrogel-Rapid Prototyping for Tissue Engineering. Biomaterials. 2012; 33(26): 6020–6041. [PubMed: 22681979]
64. Dalton PD, Klinkhammer K, Salber J, Klee D, Möller M. Direct in Vitro Electrospinning with Polymer Melts. Biomacromolecules. 2006; 7(3):686–690. [PubMed: 16529400]
65. Lu B, He Y, Duan H, Zhang Y, Li X, Zhu C, Xie E. A New Ultrahigh-Speed Method for the Preparation of Nanofibers Containing Living Cells: A Bridge towards Industrial Bioengineering Applications. Nanoscale. 2012; 4(3):1003–1009. [PubMed: 22234790]
66. Yuan S, Li Z, Song L, Shi H, Luan S, Yin J. Liquid-Infused Poly(styrene- *B* -Isobutylene- *B* -Styrene) Microfiber Coating Prevents Bacterial Attachment and Thrombosis. ACS Appl Mater Interfaces. 2016; 8(33):21214–21220. [PubMed: 27482919]
67. Bilbao-Sainz C, Chiou BS, Valenzuela-Medina D, Du WX, Gregorski KS, Williams TG, Wood DF, Glenn GM, Orts WJ. Solution Blow Spun Poly(lactic Acid)/hydroxypropyl Methyl-cellulose Nanofibers with Antimicrobial Properties. Eur Polym J. 2014; 54:1–10.
68. Bonan RF, Bonan PRF, Batista AUD, Sampaio FC, Albuquerque AJR, Moraes MCB, Mattoso LHC, Glenn GM, Medeiros ES, Oliveira JE. In Vitro Antimicrobial Activity of Solution Blow Spun Poly(lactic Acid)/polyvinylpyrrolidone Nanofibers Loaded with Copaiba (Copaifera Sp.) Oil. Mater Sci Eng, C. 2015; 48:372–377.
69. Oliveira JE, Medeiros ES, Cardozo L, Voll F, Madureira EH, Mattoso LHC, Assis OBG. Development of Poly(lactic Acid) Nanostructured Membranes for the Controlled Delivery of Progesterone to Livestock Animals. Mater Sci Eng, C. 2013; 33(2):844–849.
70. Zhuang X, Shi L, Zhang B, Cheng B, Kang W. Coaxial Solution Blown Core-Shell Structure Nanofibers for Drug Delivery. Macromol Res. 2013; 21(4):346–348.
71. Khansari S, Duzyer S, Sinha-Ray S, Hockenberger A, Yarin AL, Pourdeyhimi B. Two-Stage Desorption-Controlled Release of Fluorescent Dye and Vitamin from Solution-Blown and Electrospun Nanofiber Mats Containing Porogens. Mol Pharmaceutics. 2013; 10(12):4509–4526.
72. Oliveira JE, Mattoso LHC, Medeiros ES, Zucolotto V. Poly(lactic acid)/Carbon Nanotube Fibers as Novel Platforms for Glucose Biosensors. Biosensors. 2012; 2(4):70–82. [PubMed: 25585633]
73. Oliveira JE, Grassi V, Scagion VP, Mattoso LHC, Glenn GM, Medeiros ES. Sensor Array for Water Analysis Based on Interdigitated Electrodes Modified With Fiber Films of Poly(Lactic Acid)/Multiwalled Carbon Nanotubes. IEEE Sens J. 2013; 13(2):759–766.
74. Gupta, VB., Kothari, VK., editors. Manufactured Fibre Technology. Springer; Dordrecht, The Netherlands: 1997.
75. Tuteja A, Choi W, Ma M, Mabry JM, Mazzella SA, Rutledge GC, McKinley GH, Cohen RE. Designing superoleophobic surfaces. Science. 2007; 318:1618–1622. [PubMed: 18063796]
76. Shi L, Zhuang X, Tao X, Cheng B, Kang W. Solution Blowing Nylon 6 Nanofiber Mats for Air Filtration. Fibers Polym. 2013; 14(9):1485–1490.

77. Lee J-G, Kim D-Y, Mali MG, Al-Deyab SS, Swihart MT, Yoon SS. Supersonically Blown Nylon-6 Nanofibers Entangled with Graphene Flakes for Water Purification. Nanoscale. 2015; 7(45): 19027–19035. [PubMed: 26514169]

78. Hsiao HY, Huang CM, Hsu MY, Chen H. Preparation of High-Surface-Area PAN-Based Activated Carbon by Solution-Blowing Process for CO2 Adsorption. Sep Purif Technol. 2011; 82:19–27.

79. Tao X, Zhou G, Zhuang X, Cheng B, Li X, Li H. Solution Blowing of Activated Carbon Nanofibers for Phenol Adsorption. RSC Adv. 2015; 5(8):5801–5808.

80. Sinha-Ray S, Sinha-Ray S, Yarin AL, Pourdeyhimi B. Application of Solution-Blown 20–50 Nm Nanofibers in Filtration of Nanoparticles: The Efficient van Der Waals Collectors. J Membr Sci. 2015; 485:132–150.

81. Wang H, Zhuang X, Li X, Wang W, Wang Y, Cheng B. Solution Blown Sulfonated Poly(ether Sulfone)/poly(ether Sulfone) Nanofiber-Nafion Composite Membranes for Proton Exchange Membrane Fuel Cells. J Appl Polym Sci. 2015; 132(38):42572.

82. Wang H, Zhuang X, Tong J, Li X, Wang W, Cheng B, Cai Z. Solution-Blown SPEEK/POSS Nanofiber–nafion Hybrid Composite Membranes for Direct Methanol Fuel Cells. J Appl Polym Sci. 2015; 132(47):42843.

83. Xu X, Li L, Wang H, Li X, Zhuang X. Solution Blown Sulfonated Poly(ether Ether Ketone) nanofiber–Nafion Composite Membranes for Proton Exchange Membrane Fuel Cells. RSC Adv. 2015; 5(7):4934–4940.

84. Shi S, Zhuang X, Cheng B, Wang X. Solution Blowing of ZnO Nanoflake-Encapsulated Carbon Nanofibers as Electrodes for Supercapacitors. J Mater Chem A. 2013; 1(44):13779.

85. Jia K, Zhuang X, Cheng B, Shi S, Shi Z, Zhang B. Solution Blown Aligned Carbon Nanofiber Yarn as Supercapacitor Electrode. J Mater Sci: Mater Electron. 2013; 24(12):4769–4773.

86. Li L, Kang W, Zhao Y, Li Y, Shi J, Cheng B. Preparation of Flexible Ultra-Fine Al2O3 Fiber Mats via the Solution Blowing Method. Ceram Int. 2015; 41(1):409–415.

87. Cheng B, Tao X, Shi L, Yan G, Zhuang X. Fabrication of ZrO2 Ceramic Fiber Mats by Solution Blowing Process. Ceram Int. 2014; 40(9):15013–15018.

88. Farias RM, da C, Menezes RR, Oliveira JE, de Medeiros ES. Production of Submicrometric Fibers of Mullite by Solution Blow Spinning (SBS). Mater Lett. 2015; 149:47–49.

89. Rotta M, Zadorosny L, Carvalho CL, Malmonge JA, Malmonge LF, Zadorosny R. YBCO Ceramic Nanofibers Obtained by the New Technique of Solution Blow Spinning. Ceram Int. 2016; 42(14): 16230–16234.

90. Costa DL, Leite RS, Neves GA, Santana LNdL, Medeiros ES, Menezes RR. Synthesis of TiO2 and ZnO Nano and Submicrometric Fibers by Solution Blow Spinning. Mater Lett. 2016; 183:109–113.

91. Gonzalez-Abrego M, Hernandez-Granados A, Guerrero-Bermea C, Martinez de la Cruz A, Garcia-Gutierrez D, Sepulveda-Guzman S, Cruz-Silva R. Mesoporous Titania Nanofibers by Solution Blow Spinning. J Sol-Gel Sci Technol. 2016; 2016:1–7.

92. Giannatsis J, Dedoussis V. Additive Fabrication Technologies Applied to Medicine and Health Care: A Review. Int J Adv Manuf Technol. 2009; 40(1–2):116–127.

93. Zeng W, Shu L, Li Q, Chen S, Wang F, Tao X-M. Fiber-Based Wearable Electronics: A Review of Materials, Fabrication, Devices, and Applications. Adv Mater. 2014; 26(31):5310–5336. [PubMed: 24943999]

94. Tutak W, Kaufman G, Gelven G, Markle C, Maczka C. Uniform, Fast, High Concentration Delivery of Bone Marrow Stromal Cells and Gingival Fibroblasts by Gas-Brushing. Biomed Phys Eng Express. 2016; 2(3):035007.

95. Veazey WS, Anusavice KJ, Moore K. Mammalian Cell Delivery via Aerosol Deposition. J Biomed Mater Res, Part B. 2005; 72B(2):334–338.

96. Pehlivaner Kara MO, Ekenseair AK. *In Situ* Spray Deposition of Cell-Loaded, Thermally and Chemically Gelling Hydrogel Coatings for Tissue Regeneration. J Biomed Mater Res, Part A. 2016; 104(10):2383–2393.

97. Demirel MC, Cetinkaya M, Pena-Francesch A, Jung H. Recent Advances in Nanoscale Bioinspired Materials: Recent Advances in Nanoscale Bioinspired Materials. Macromol Biosci. 2015; 15(3): 300–311. [PubMed: 25476469]

98. Khansari S, Sinha-Ray S, Yarin AL, Pourdeyhimi B. Biopolymer-Based Nanofiber Mats and Their Mechanical Characterization. Ind Eng Chem Res. 2013; 52(43):15104–15113.

99. Sett S, Stephansen K, Yarin AL. Solution-Blown Nanofiber Mats from Fish Sarcoplasmic Protein. Polymer. 2016; 93:78–87.

100. da Silva Parize DD, de Oliveira JE, Foschini MM, Marconcini JM, Mattoso LHC. Poly(lactic Acid) Fibers Obtained by Solution Blow Spinning: Effect of a Greener Solvent on the Fiber Diameter. J Appl Polym Sci. 2016; 133(18):43379.

101. Zhuang X, Shi L, Jia K, Cheng B, Kang W. Solution Blown Nanofibrous Membrane for Microfiltration. J Membr Sci. 2013; 429:66–70.

102. Mahalingam S, Edirisinghe M. Forming of Polymer Nanofibers by a Pressurised Gyration Process. Macromol Rapid Commun. 2013; 34(14):1134–1139. [PubMed: 23749758]

103. Yetisen AK, Qu H, Manbachi A, Butt H, Dokmeci MR, Hinestroza JP, Skorobogatiy M, Khademhosseini A, Yun SH. Nanotechnology in Textiles. ACS Nano. 2016; 10(3):3042–3068. [PubMed: 26918485]

104. Tutak W, Gelven G, Markle C, Palmer X-L. Rapid Polymer Fiber Airbrushing: Impact of a Device Design on the Fiber Fabrication and Matrix Quality. J Appl Polym Sci. 2015; 132(47): 42813.

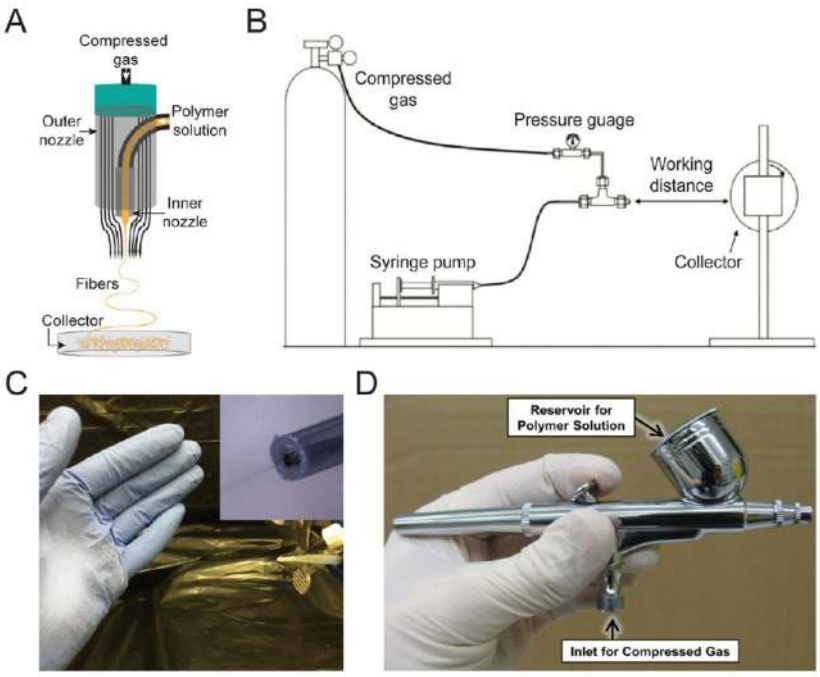

Figure 1.

(A) Schematic for a solution blow spinning device showing concentric nozzles. Adapted with permission from ref 1. Copyright 2015 American Chemical Society. (B) A general solution blow spinning process diagram with rolling collector. Adapted with permission from ref 3. Copyright 2009 Wiley-VCH. (C) Image of direct deposition of poly(styrene-*block*-isoprene-*block*-styrene) block copolymer fibers using a homemade solution blow spinning device. The homemade device was made from a transfer pipet and a flat tipped 18G needle (inset). Adapted with permission from ref 1. Copyright 2015 American Chemical Society. (D) A commercial airbrush used for solution blow spinning. Adapted with permission from ref 2. Copyright 2013 Elsevier.

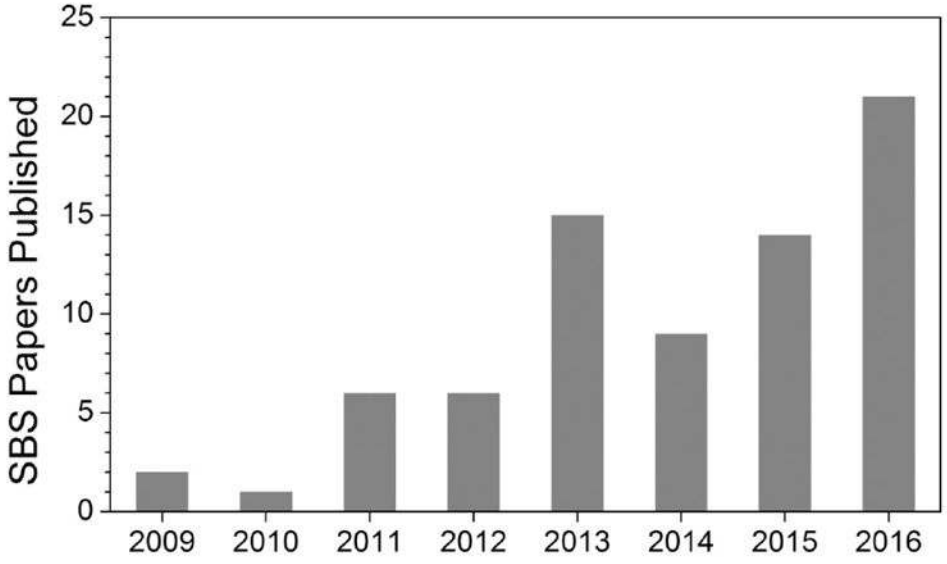

Figure 2.

Number of publications on solution blow spinning and related topics has increased since its widespread exposure began in 2009. Data for 2016 is current as of September.

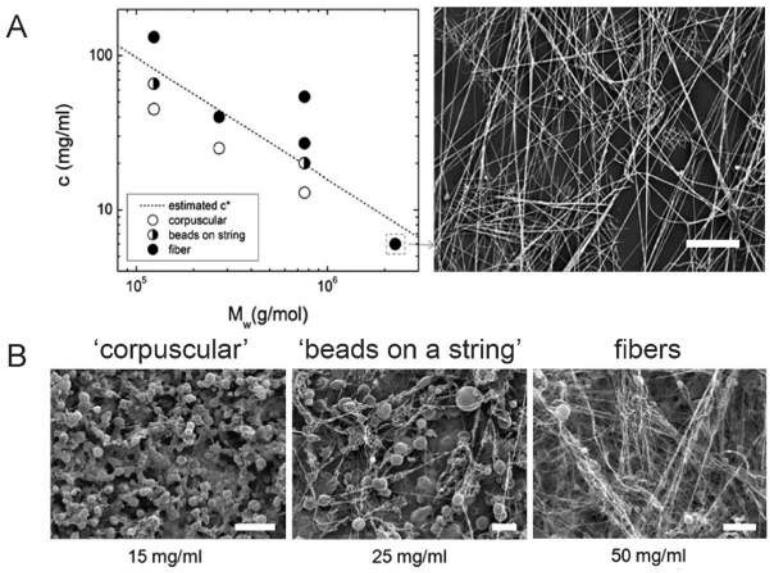

Figure 3.

(A) Plot indicating morphology of poly(methyl methacrylate) (PMMA) sprayed using a solution blow spinning (SBS) apparatus at various concentrations and molecular weights. The estimated overlap concentration (c^*) is indicated by the dashed line. Scanning electron microscopy (SEM) image of PMMA fibers formed at high molecular weight but below overlap concentration. Scale bar represents 50 μm. (B) SEM images of 50/50 wt % PMMA/1H,1H,2H,2H-heptadecafluorodecyl polyhedral oligomeric silsesquioxane (PMMA: M_w = 593 kDa, PDI = 2.69) blends sprayed using an SBS apparatus at increasing concentrations of PMMA in solution. Scale bars represent 50, 100, and 50 μm, respectively. Adapted with permission from ref 19. Copyright 2011 Elsevier.

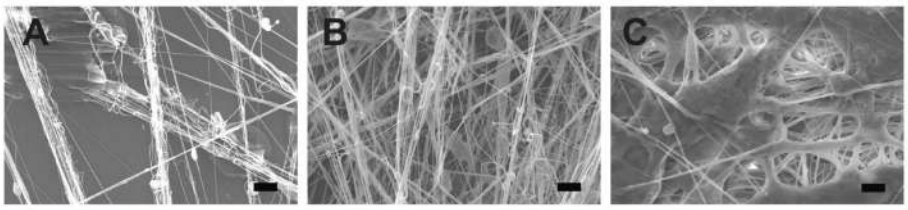

Figure 4.

(A–C) Scanning electron microscopy (SEM) images of fiber morphologies produced by solution blow spinning 10% w/v poly(lactic-*co*-glycolic acid) in acetone at CO_2 flow rates of 10 SCFH (A), 13 SCFH (B), and 15 SCFH (C). Scale bars correspond to 20 μm. Adapted with permission from 5. Copyright 2014 American Chemical Society.

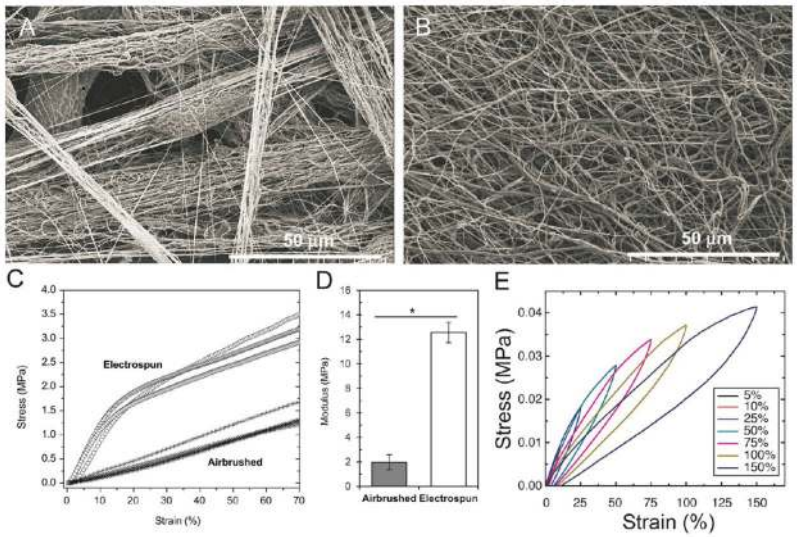

Figure 5.

Morphology, Young's modulus, and cyclic testing of solution blow spinning (SBS) fibers. (A) Fiber bundles produced by SBS of a 4 wt % polymer solution of poly(caprolactone) (PCL) (80 kDa) in chloroform. (B) Fibers produced by electrospinning a 4 wt % polymer solution of PCL (80 kDa) in 3:1 chloroform:methanol by mass. A, B adapted with permission from ref 2. Copyright 2013 Elsevier. (C) Comparison of stress–strain curves for PCL (80 kDa) fiber mats fabricated using electrospinning and SBS. (D) Young's modulus for fiber mats produced using SBS and electrospinning PCL fibers. C, D adapted with permission from ref 2. Copyright 2013 Elsevier. (E) Stress/strain cycling curves at varying maximum strain values for poly(styrene-*block*-isoprene-*block*-styrene) fiber mats fabricated by SBS. Adapted with permission from ref 1. Copyright 2015 American Chemical Society.

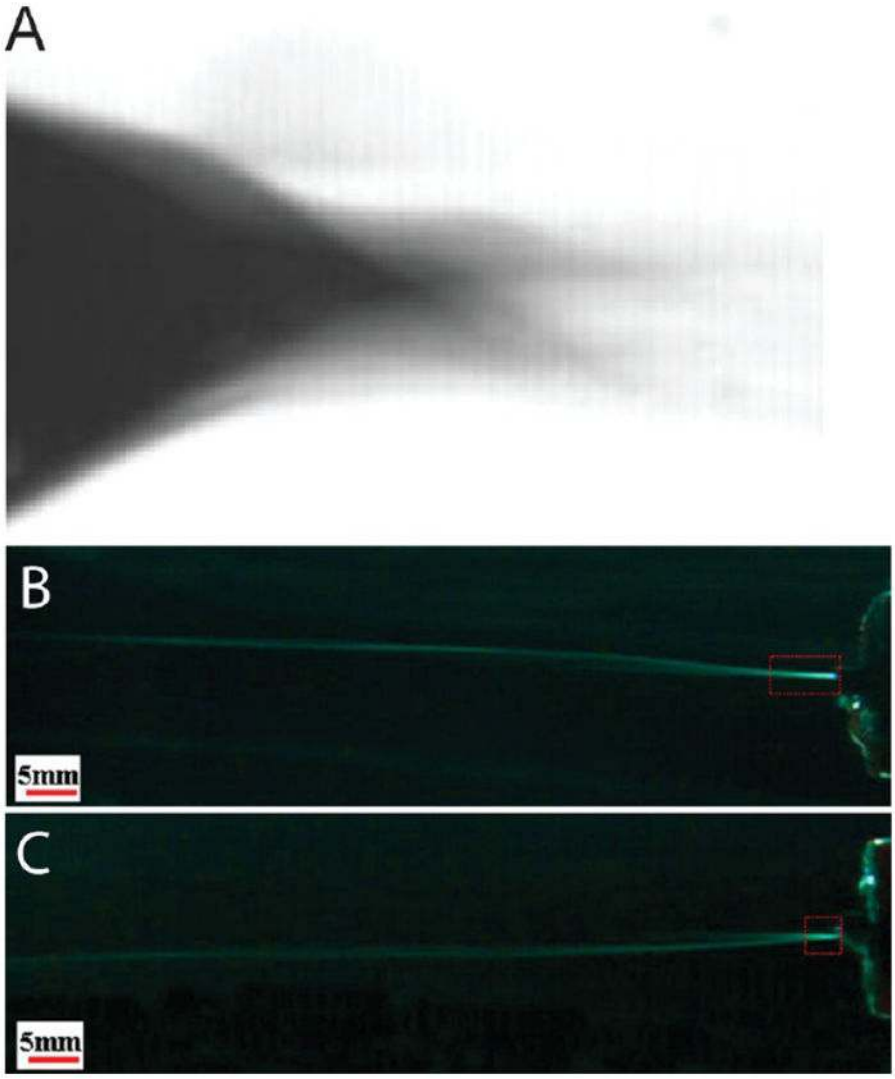

Figure 6.

Images showing the effects of turbulence on polymer jets used for solution blow spinning (SBS). (A) High-speed photograph of a polymer solution cone forming at the tip of a SBS device. Adapted with permission from ref 3. Copyright 2009 Wiley-VCH. (B, C) High-speed photograph comparing the length of the straight region (in red box) of the polymer jet produced by SBS at gas pressures of 1.121 atm (B) and 1.363 atm (C). Adapted with permission from ref 46. Copyright 2014 American Chemical Society.

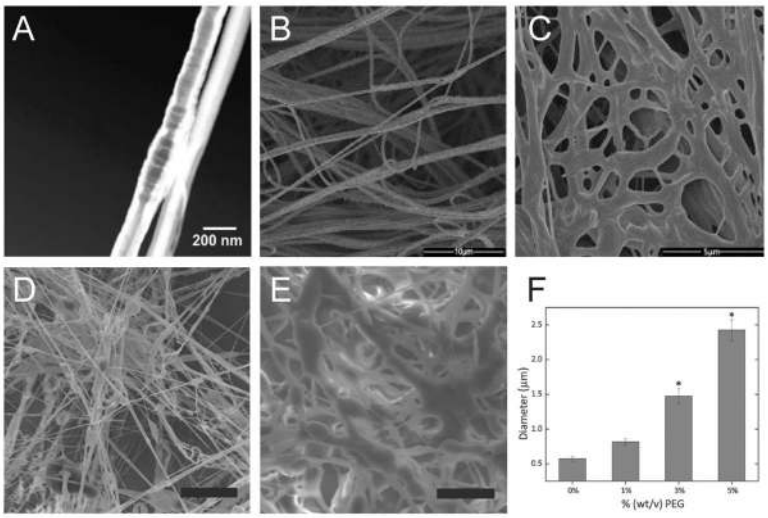

Figure 7.

Various multicomponent fibers produced by solution blow spinning (SBS). (A) Transmission electron microscopy images of core–shell fibers produced by SBS from a 1:1 blend of poly(lactic acid) and poly(ethylene glycol) (PEG) at 6% w/v in solution. Adapted with permission from ref 49. Copyright 2013 Wiley-VCH. (B, C) Scanning electron microscopy (SEM) images of fibers produced by SBS from a 1:1 blend of chitosan and poly(vinyl alcohol) at 8% w/v in solution with 7% ethylene glycol diglycidyl ether cross-linker (relative to mass of polymer). SEM images were taken after drying in a vacuum oven for 3 h (B) and after drying then swelling in saline solution for 8 h (C). Adapted with permission from ref 56. Copyright 2014 Elsevier. (D) Fibers produced by SBS from a 10% w/v poly(lactic-*co*-glycolic acid) (PLGA) in acetone solution. (E) Fibers produced by SBS from a 10% w/v PLGA, 5% w/v PEG blend in solution. (F) Fiber diameter produced by SBS from a 10% w/v PLGA solution increases with increasing PEG blend content. Adapted with permission from ref 57. Copyright 2015 Wiley-VCH.

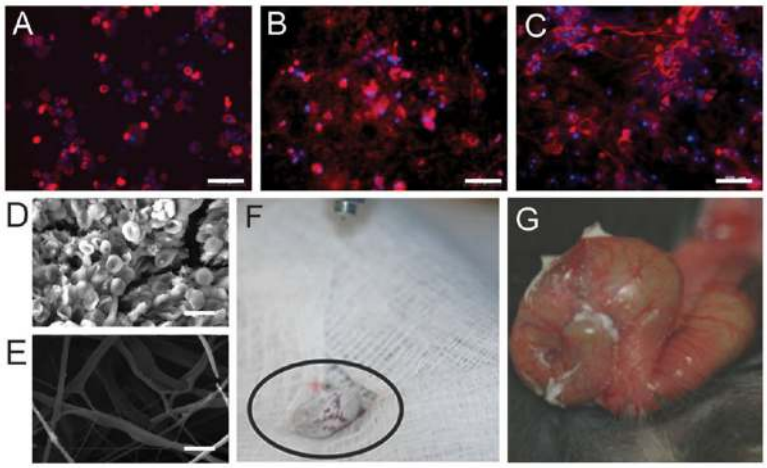

Figure 8.

Biomaterials applications of solution blow spinning (SBS). A–C) Fluorescent microscopy images showing MSCs cultured on a flat cell culture control surface (A), polyvinylidene fluoride-trifluoroethylene copolymer (VDF-TeFE) fibers produced by electrospinning (B), and VDF-TeFE fibers produced by SBS (C). Scale bars represent 100 μm. Adapted with permission from ref 38. Copyright 2016 Elsevier. (D, E) Field emission scanning electron microscopy (FESEM) images showing blood cell and platelet attachment to poly(styrene-*b*-isobutylene-*b*-styrene) (SIBS) fibers (D) and SIBS fibers infused with silicon oil (E) after incubation with whole blood. Scale bars represent 10 μm. Adapted with permission from ref 66. Copyright 2016 American Chemical Society. (F) Intestinal anastomosis being coated in fibers produced by SBS from a poly(lactic-*co*-glycolic acid) (PLGA) and poly(ethylene glycol) (PEG) blend. (G) Intestinal anastomosis 2 min after being coated showing the thermal transition of PLGA–PEG fibers. (F, G) adapted with permission from ref 57. Copyright 2015 Wiley-VCH.

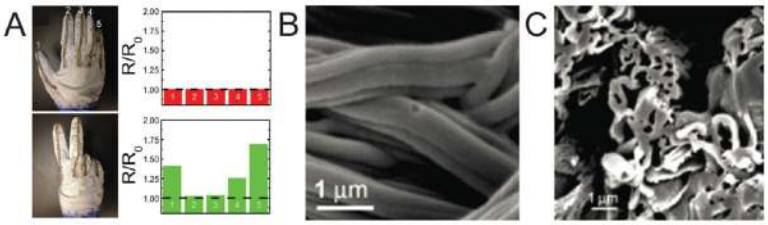

Figure 9.

Composite and postprocessing techniques enabled by solution blow spinning (SBS). (A) Glove coated in poly(styrene-*block*-isoprene-*block*-styrene) elastomeric fibers patterned with conductive bands of silver nanoparticles showing resistance measured across each line corresponding to hand gestures. Adapted with permission from ref 1. Copyright 2015 American Chemical Society. (B, C) Side (B) and cross section (C) of carbon tubes processed from core–shell poly(methyl methacrylate)-poly(acrylonitrile) fibers produced by SBS. Adapted with permission from ref 51. Copyright 2010 Elsevier.

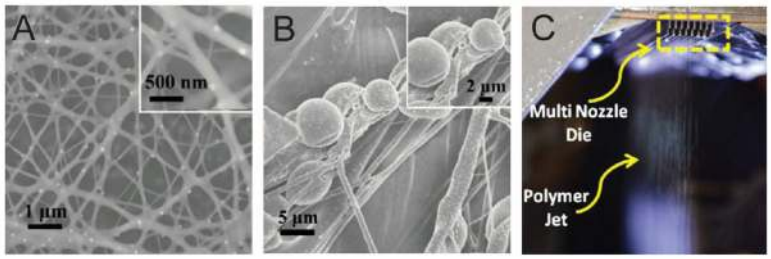

Figure 10.

Future directions for solution blow spinning (SBS) research. (A, B) Images of nanofibers produced by SBS from a 15% polyvinylpyrrolidone solution in fetal bovine serum sprayed without (A) and with (B) mouse renal epithelial cells in the solution. Adapted with permission from ref 65. Copyright 2012 RSC Publishing. (C) Multinozzle SBS process using a die with 41 nozzles per row and 8 rows. Adapted with permission from ref 27. Copyright 2016 American Chemical Society.

Table 1

Biodegradable Polymers and Solvent Combinations Used for Solution Blow Spinning

polymer	solvent	concentration (% w/v)	Gas Pressure (psi)	reference
PCL	chloroform	8	35	2
PLA	chloroform/acetone, chloroform/methanol	6	35, 29–58	2, 26
PLGA	acetone	10	N/A	5

Table 2

Biopolymer and Solvent Combinations Used for Solution Blow Spinning

polymer	solvent	concentration (wt %)	gas pressure (psi)	reference
bovine serum albumin/poly(vinyl alcohol)	water	10/10	29	98
cellulose	LiCl/dimethylacetamide (DMAc)	2	36	50
cellulose/poly(ethylene oxide)	LiCl/DMAc	2/10	36	50
cellulose acetate/polyacetonitrile	*N*,*N*-dimethylacetamide (DMF)	5/5	29	98
chitosan/poly(vinyl alcohol)	formic acid	3.2/3.2	72	56
fish sarcoplasmic protein/nylon-6	formic acid	1.75–17.5/1.75–17.5	60	99
lignin	formic acid	5–14	29	98
hydroxypropyl methylcellulose/poly(lactic acid)	trifluoroethanol	9	80	67
silk sericin/nylon-6	formic acid	12/12	29	98
soy protein/nylon-6	formic acid	9/14	N/A	52
zein/nylon-6	formic acid	9–22/11–13	29	98

Table 3

Polymer–Composite Mixtures Used for Solution Blow Spinning

polymer–composite mixture	solvent	concentration (wt %)	gas pressure (psi)	reference
$AlCl_3 \cdot 6H_2O$/silica particles/PVA	water	15/2/.4	1–10	86
$Al(NO_3) \cdot 9H_2O/Si(OC_2H_5)_4$/PVC	THF	N/A/10	40	88
PCL/zirconium-modified amorphous calcium phosphate (Zr-ACP)	chloroform	4/0–20	30–40	59
PLA/carbon nanotubes	chloroform/acetone	6/0–3	58	72
PLA/nanobioactive glass	dimethyl carbonate	3–13/4–8	20	41
PLA/Zr-ACP	acetone	8/0–20	30–40	59
PMMA/Zr-ACP	acetone	10/0–20	30–40	59
PVP/$ZrOCl_3$	water	2–5/9–15	6–17	87
PVP/YBCO	methanol/acetic acid/propionic acid	4/11	19	89